Molecular Crystals and Liquid Crystals

Publication details, including instructions for authors and subscription information:
http://www.tandfonline.com/loi/gmcl20

Backflow and Dynamic Behavior of Nematic Liquid Crystals in the Modulated Electric Field

Shouping Tang [a] & Jack Kelly [a]

[a] Liquid Crystal Institute, Kent State University, Kent, Ohio, USA

Version of record first published: 22 Sep 2010

To cite this article: Shouping Tang & Jack Kelly (2008): Backflow and Dynamic Behavior of Nematic Liquid Crystals in the Modulated Electric Field, Molecular Crystals and Liquid Crystals, 490:1, 27-42

To link to this article: http://dx.doi.org/10.1080/15421400802305798

Mol. Cryst. Liq. Cryst., Vol. 490, pp. 27–42, 2008

ISSN: 1542-1406 print/1563-5287 online
DOI: 10.1080/15421400802305798

Backflow and Dynamic Behavior of Nematic Liquid Crystals in the Modulated Electric Field

Shouping Tang and Jack Kelly
Liquid Crystal Institute, Kent State University, Kent, Ohio, USA

We have investigated backflow and dynamic behavior of a homogeneously aligned liquid crystal cell in the modulated electric field. We quantitatively describe the dynamic behavior of director, flow velocity, and fluid displacement. The numerical calculation shows the whole dynamic process of director and flow in the modulated electric field. We also show an important phenomenon, reverse switch for nematic liquid crystals in the modulated electric field, which has never been mentioned before.

Keywords: backflow; direct flow; dynamic behavior; fluid displacement; fluid shift; modulated electric field; reverse flow; reverse switch

1. INTRODUCTION

Since the importance of hydrodynamic flow in the dynamic response of liquid crystal devices was shown by van Doorn [1] and Berreman [2] in their illustrations of the tipping over of director and optical bounce due to backflow in TN cell, it has been recognized that liquid crystal flow during director reorientation has a significant impact on switching dynamics. Flow-induced reorientation of the director in the middle region of a TN and the so-called *optical bounce* observed in the transmission of a TN cell between polarizers [3,4] are two primary examples. Although the dynamic properties of nematic liquid crystals with consideration of backflow were illustrated in many articles for different director configurations, such as twisted cells [1–10] and untwisted cells [11–17], it is worthy to notice that, all these investigations are restricted to the simple switching scheme, switching ON or OFF. However, the additional consequences of flow and the dynamic

Address correspondence to Shouping Tang, Liquid Crystal Institute, Kent State University, Kent, OH 44242, USA. E-mail: sptang66@hotmail.com

behavior that result from the complicated switching scheme, such as the modulated signals, have received little attention and are poorly understood. In fact, a lot of LC devices work under the modulated signals with fast ON and OFF switching. Understanding of the backflow and dynamic behavior with different switching schemes may lead to the improvement of device switching characteristics.

In this article, we present our numerical investigation on backflow and dynamic behavior of a homogeneously aligned liquid crystal cell in the modulated electric field. The numerical calculation shows the whole dynamic process of director and flow in the modulated electric field. We quantitatively describe the dynamic behavior of director $\hat{\mathbf{n}}(z,t)$, flow velocity $\vec{v}(z,t)$, the net flow velocity $\langle v \rangle$ (average velocity of flow within a modulated period) and the displacement of fluid (S_{on} for ON and S_{off} for OFF). Especially, reverse-switch, which is never mentioned before, is an important phenomenon for nematic liquid crystals in the modulated electric field. Realizing the reverse-switch and the corresponding reverse flow may be very crucial for studying dynamic properties of liquid crystals with the complicated switching schemes, such as the modulated signals.

2. LIQUID CRYSTAL CELL AND COMPUTER SIMULATION

A homogeneously aligned liquid crystal cell filled with E7 ($K_{11} = 11.7 \times 10^{-12}\,\mathrm{J/m}$, $K_{33} = 19.5 \times 10^{-12}\,\mathrm{J/m}$, $\varepsilon_{\parallel} = 19.6$, $\Delta_{\varepsilon} = 14.5$, $\alpha_1 = -21.2\,\mathrm{mPa \cdot s}$, $\alpha_2 = -281.8\,\mathrm{mPa \cdot s}$, $\alpha_3 = -1.0\,\mathrm{mPa \cdot s}$, $\alpha_4 = 224.7\,\mathrm{mPa \cdot s}$, $\alpha_5 = 92.1\,\mathrm{mPa \cdot s}$, $\alpha_6 = -190.6\,\mathrm{mPa \cdot s}$, $T = 20.4^{\circ}\mathrm{C}$) [18] was used in the investigation. The cell thickness is 21 μm, and pretilt angle is 2°. In addition, we also investigated the influences of cell thickness and pretilt angle on the average velocity of flow in the modulated electric field. The used cell thickness and pretilt angle are: 20, 21, and 22 μm of cell thickness with a 2° of pretilt angle, and 1, 2, and 3° of pretilt angle with a 21 μm of cell thickness. In the calculation, there are six Leslie viscosities involved, and the correct result depends on the accuracy of these viscosities, as well as that of cell thickness and pretilt angle.

We performed numerical simulation based on Ericksen–Leslie–Parodi (ELP) theory [19–23] for the applied voltage $U = 10\,\mathrm{V}$. We assume that $\hat{\mathbf{n}} = \{\cos\theta(z,t), 0, \sin\theta(z,t)\}$ is in the xz plane, and that the hydrodynamic flow has only the x component, $\mathbf{v} = \{v(z,t), 0, 0\}$. We neglect the flow inertia term because the flow relaxation time $\tau_v \approx \rho h^2/\pi^2\alpha_4 \sim 1\,\mu\mathrm{s}$ is much shorter than the director relaxation times $\tau_{on} \approx (\alpha_3 - \alpha_2)h^2/\varepsilon_0(\varepsilon_{\parallel} - \varepsilon_{\perp})U^2 \sim 10\,\mathrm{ms}$ and $\tau_{off} \approx (\alpha_3 - \alpha_2)$

$h^2/\pi^2 K_1 \sim 1$s, and write the director equation and flow equation as:

$$\gamma_1 \frac{\partial \theta}{\partial t} = (h_z \cos\theta - h_x \sin\theta) - (\alpha_3 \cos^2\theta - \alpha_2 \sin^2\theta)\frac{\partial v}{\partial z}, \tag{1}$$

$$\begin{aligned}(\alpha_3 \cos^2\theta - \alpha_2 \sin^2\theta)\frac{\partial \theta}{\partial t} + \frac{1}{2}\Bigg[\frac{1}{2}\alpha_1 \sin^2 2\theta \\ + (\alpha_5 - \alpha_2)\sin^2\theta + \alpha_4 + (\alpha_3 + \alpha_6)\cos^2\theta\Bigg]\frac{\partial v}{\partial z} = c(t),\end{aligned} \tag{2}$$

where h is the molecular field defined as the functional derivative of free energy density [24], and $c(t)$ is the time-dependent integration constant that does not depend on z and is determined from the boundary condition $v(z=0) = v(z=h) = 0$. We solve Eqs. (1, 2) using an implicit Crank–Nicolson scheme for the time derivatives.

For a modulated electric field, the electric signal is controlled by setting triggers in the numerical implementation, which control the applied voltage and the frequency in the calculation. When the vibrations of director and flow are stable after several modulation periods, the average velocity $\langle v \rangle$ over a modulation period is calculated as

$$\langle v \rangle = \frac{\int_T v_x(z,t)dt}{T}, \tag{3}$$

where T is the period of a modulated signal. The number of modulation periods needed for the vibrations of director and flow to reach stable depends on the frequency of electric signal. In order to get accurate numerical solution, a small time step is needed to make sure the convergence in the calculation of average flow velocity.

3. BACKFLOW AND DYNAMIC BEHAVIOR OF DIRECTOR

In the modulated electric field, backflow was created by a high frequency of voltage U = 10 V, modulated with a frequency f_m. The carrier frequency f and modulation frequency f_m can be varied. The duty ratio defined as the duration of the field ON to the total duration of the field cycle was 50%. We numerically investigated the backflow and dynamic properties of liquid crystals for the carrier frequency 10 kHZ and the modulation frequency between 1 HZ to 100 HZ.

In our cell, such a stable vibration is establishing after elapsing of $\sim$200 ms of applied signal. When the dynamic procedure of director reorientation and flow is well established (time frame 300–400 ms of applied signal), the flow and dynamic director within a modulation

period with the modulation frequency 10 HZ are shown in Fig. 1. The flow and the variation of flow around the intermediate regions are relatively big, while the flow is relatively small in the middle region and the regions next to surfaces, and is zero at the middle and the surfaces (Fig. 1a). Oppositely, the variation of director in the intermediate regions is relatively small, while the variation of director in the middle region and the regions next to surfaces is relatively big (Fig. 1b). The

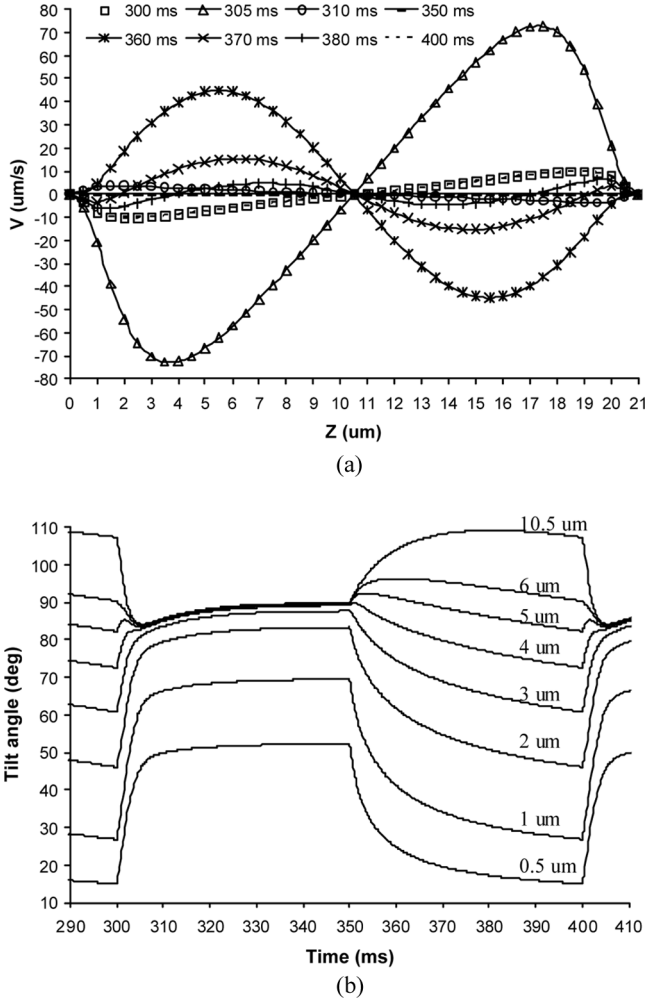

FIGURE 1 Flow and director within a modulation period (time frame from 300 ms to 400 ms) with modulation frequency $f_m = 10$ HZ; (a) flow profile, (b) dynamic director profile.

dynamic behavior of director and flow within a modulation period can be illustrated in Fig. 2. At the beginning of a modulation period (at t = 300 ms), the cell is switched ON. Director in the middle layer is still in the flipped-over position (the reorientation angle is $\sim 107^{\circ}$) and the electric field forces the director to rotate clockwise to align parallel to the field while the director next to surfaces rotates counterclockwise (Fig. 2b). This reorientation of the director induces large reverse flow (Fig. 2c), which in turn reorients the director in the middle down to $\sim 84^{\circ}$ (time frame 300–306 ms, Fig. 2b). Then, the director in middle rotates counterclockwise to align along the field and reaches $\sim 90^{\circ}$

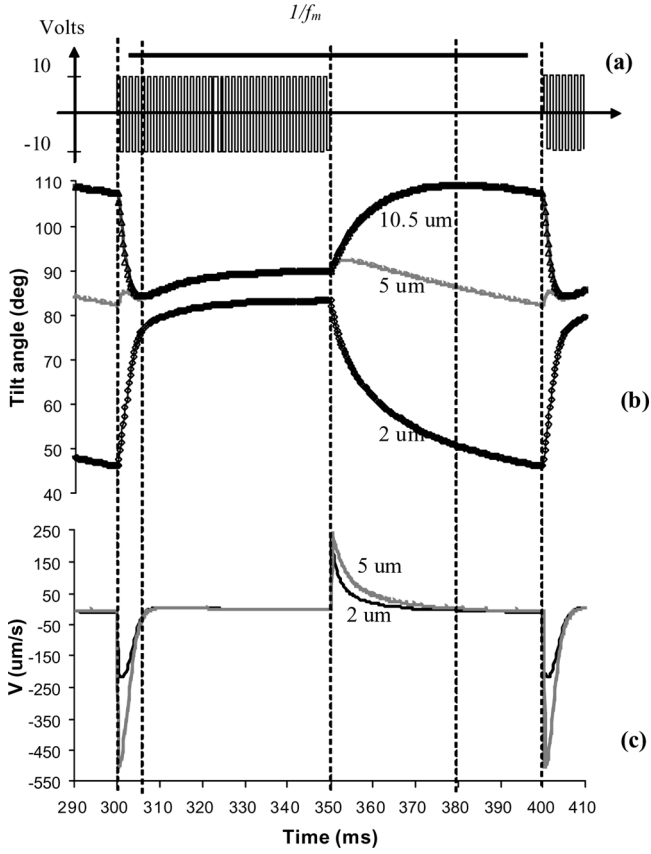

FIGURE 2 Illustration of director and flow within a modulation period (from 300 ms to 400 ms) under a high frequency of voltage U = 10 V, modulated with a frequency $f_m = 10$ HZ; (a) Scheme of applied signal (U = 10 volts, $f_m = 10$ HZ), (b) director at 2, 5 and 10.5 um, and (c) flow at 2 um and 5 um.

reorientation, thus inducing a very small flow (time frame 306–350 ms). When the field is switched OFF (at $t = 350$ ms), the director next to surfaces rotates clockwise due to elastic torque in the regions next to surfaces and creates a direct flow. This director flow induces the director in the middle region to flip over 90° up to ~109° (time frame 350–380 ms). Direct flow vanishes when director in the middle layer starts to relax towards the initial state and reaches ~107° of reorientation at $t = 400$ ms. At this time the field is switched ON again, the next modulation period begins, and the dynamic procedure repeats. Therefore, the flow observed under modulated signal consists of two major parts: (a) large reverse flow during the first half of the modulation period when the cell is switched ON, (b) direct flow during second half of the modulation period when the cell is switched OFF. Thus, the direction of flow under modulated signal is completely different from the situation: switch OFF is followed by switch ON pulse only after director reaches its equilibrium state. In this situation, we observe direct flow when the cell is switched ON (Fig. 3a), and direct flow and small reverse flow when the voltage is OFF (Fig. 3b). For the modulated signal, we observe reverse flow when the cell is switched ON and direct flow when the voltage is OFF (see Fig. 1a and Fig. 2c).

The above illustration is about the dynamic procedure within a modulation period when the stable vibration is well established after elapsing of ~200 ms of applied signal. The whole dynamic procedure including the prophase when the modulated electric signal is applied is shown in Fig. 4. When the cell is first switched ON, the rotation of the director due to the applied electric field induces the direct flow (time frame 0–50 ms). At $t = 50$ ms, the cell is switched OFF, and the director near substrates relaxes back due to elastic torque. This leads to a relatively large director flow and it pushes the director in the middle layers region flip over to an angle bigger than 90°. The director in the middle layers region flips over to a maximum point, and then relaxes back (time frame 50–100 ms). Just before the director of the middle region passses through the normal direction, the second modulation period begins. In the second modulation period, the electric field reversely switches the director in the middle region and the director rotates very quickly, this leads a very large reverse flow pulse (time frame 100–150 ms). When the cell is switching OFF, the director near substrates relaxes back and leads a relatively large direct flow, and it pushes the director in the middle layers filp over again. The director flips over to a maximum point and then relaxes back (time frame 150–200 ms). After several of modulation periods, the stable vibration of the director and flow is well established.

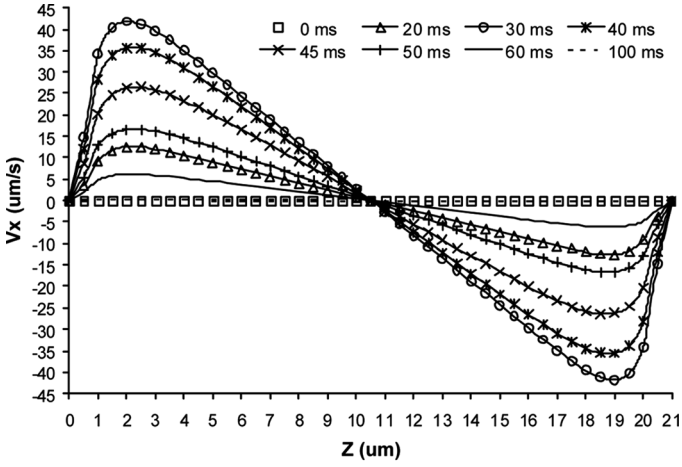

(a)

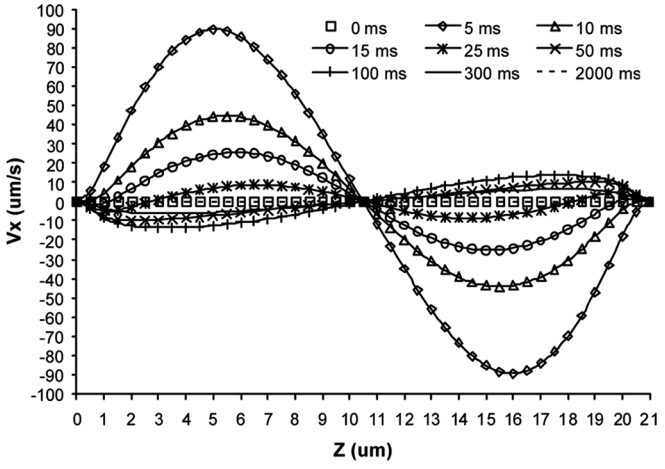

(b)

FIGURE 3 Dynamic profiles of backflow when the cell is switched between 0 V and 10 V; (a) switched ON and (b) switched OFF.

In general, the director near substrates is switched ON and then relaxes back, while the director of middle region is REVERSELY switched ON and then flips over. The flow in the intermediate regions consists of the corresponding two parts. The first is the large reverse flow due to the REVERSELY switching of the middle director and the switching of director next to surfaces. The second is the direct flow due to rotation of the director next to the substrates (relaxation of

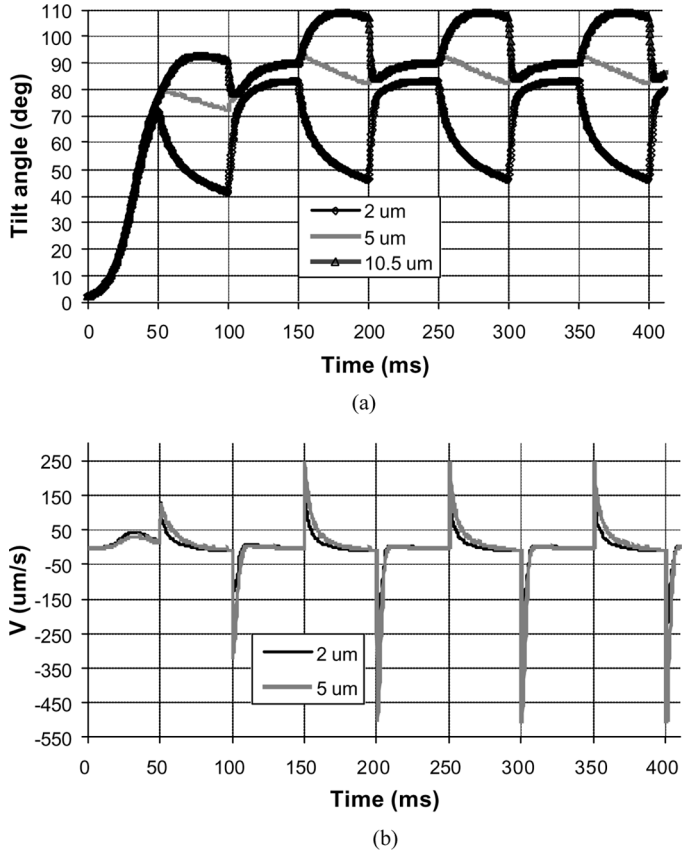

FIGURE 4 The dynamic procedure when the modulated electric field (10 V, $f = 10$ kHZ, and $f_m = 10$ HZ) is applied; (a) dynamic behavior of director and (b) backflow.

director due to strong elastic torque), which leads to the flipping over of middle director.

The dynamic behavior of the director is similar for high modulation frequency. For example, at $f_m = 100$ HZ, there exists reverse switch (Fig. 5a). But the amplitude of director vibration around 90 degree is smaller than that for $f_m = 10$ HZ of the modulation frequency, i.e., the vibration of director around 90° will decrease with the increase of the modulation frequency. In addition, at a high modulation frequency, a large number of signal periods are needed to reach the stable vibration of director. With the very low modulation frequency, the

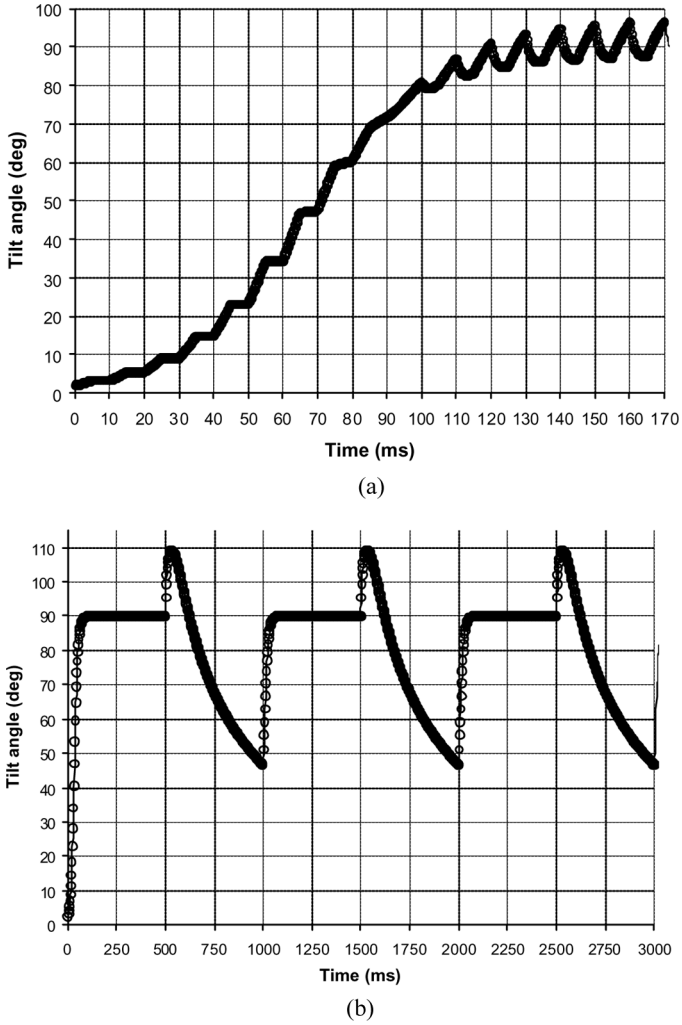

FIGURE 5 Dynamic profiles of the middle director with modulation frequency; (a) $f_m = 100\,\text{HZ}$ and (b) $f_m = 1\,\text{HZ}$.

reverse switching does not exist. Figure 5b shows the dynamic profile of the middle director at 1 HZ of modulation frequency. We can see that, there is enough time for the director at the middle to relax to below 90° from the flipping over, therefore the reverse switch does not exist.

4. NET FLOW VELOCITY AND SHIFT OF LIQUID CRYSTAL FLUID

In the above, we have shown the whole dynamic procedures of director and flow in the modulated electric field. After the director vibration reaches stable, the flow consists of two major parts: large reverse flow during the first half of the modulation period (ON) and direct flow during the second half of the modulation period (OFF). The average flow velocity $\langle v \rangle$ is the net velocity within a modulation period (see Eq. (3)). In the calculation of $\langle v \rangle$, there are two things that need attention. The first is to make sure the vibration has reached stable before calculating the average over a modulation period, the second is to use enough small time step in the numerical calculation in order to get an accurate solution. As an illustrative example, Fig. 6 shows the calculation process for getting a relatively accurate numerical solution for the $\langle v \rangle$ with modulation frequency 100 HZ. From Fig. 6 we know that $v(z)$ should be averaged within a modulation period after 310 ms (Fig. 6a) and time step should be less than 0.01 ms (Fig. 6b). We repeated the same calculation process in all of the calculations for different modulation frequencies in order to get the relatively accurate numerical solutions. The calculated profiles of $\langle v \rangle$ with different modulation frequencies are shown in Fig. 7a. It is obvious that the maximum $\langle v \rangle$ is near substrates (around 2 um or 19 um). We plot $\langle v \rangle$ at the positions 2 um and 19 um as the function of modulation frequency (see Fig. 7b), and get that the maximum $\langle v \rangle$ is less than 3.0 um/s and it occurs around the modulation frequency 5 HZ.

The thickness of cell and pretilt angle can give important effects on the switching speed. Therefore, the average flow velocity $\langle v \rangle$ may be different with different cell thickness and pretilt angle. The numerical results in Fig. 8 show that the shape of profile for $\langle v \rangle$ doesn't have the obvious change with a little variation of cell thickness and pretilt angle. The amplitude of $\langle v \rangle$ has a little change with different cell thickness and pretilt angle. The average flow velocity $\langle v \rangle$ for a thin cell is bigger than that for a thick cell (Fig. 8a), and the $\langle v \rangle$ with a small pretilt angle is bigger than that with a big pretilt angle (Fig. 8b).

We have shown the flow direction in the situation that switch-OFF is followed by switch-ON pulse only after director reaches its equilibrium state (see Fig. 3). In this situation, the shifts of liquid crystal fluid in the processes of switched ON or OFF are shown in Fig. 9a. The shift of fluid in ON is not same as the shift in OFF, and therefore there is a net shift. For the modulated electric field, the director and flow vibrate in each cycle with the field switched ON and switched OFF. According to the flow average velocity $\langle v \rangle$ (Fig. 7a), we can obtain

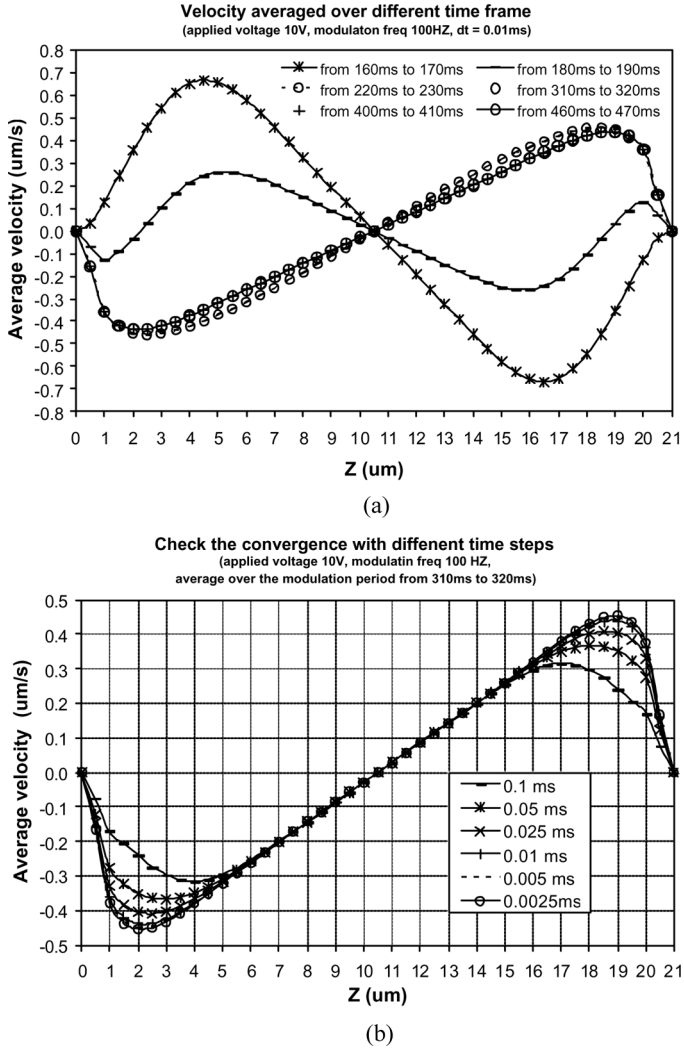

FIGURE 6 Get the relatively accurate numerical solution for average velocity $\langle v \rangle$; (a) the velocity averaged over different time fames, (b) convergence of numerical calculation with different size of time step.

the shift of liquid crystal fluid within a period of modulation signal (Fig. 9b). In Fig. 9b, the net shift of fluid at $f_m = 0\,\text{HZ}$ is equal to the shift in the situation: switch-OFF is followed by switch-ON pulse only after director reaches its equilibrium state. From the profile of fluid

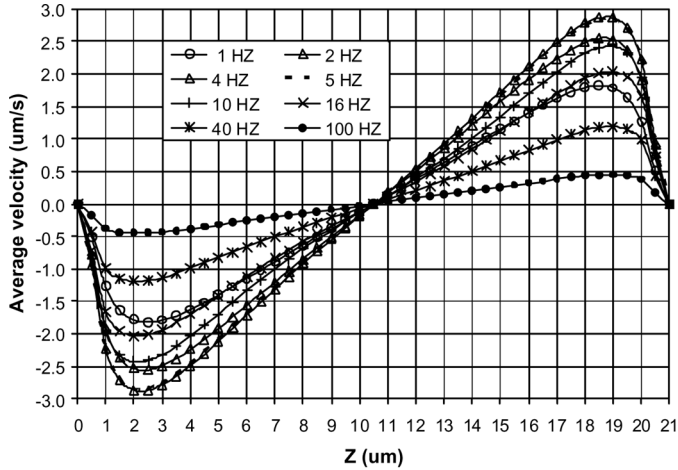

(a)

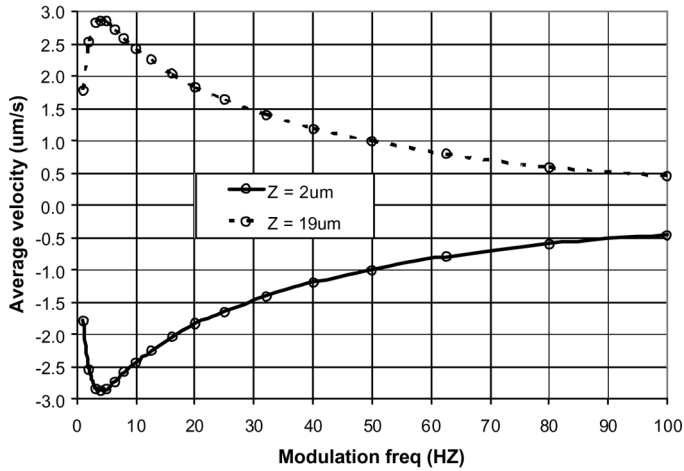

(b)

FIGURE 7 The average flow velocity $\langle v \rangle$ within a modulation period; (a) profiles of average velocity $\langle v \rangle$ with different modulation frequencies f_m, (b) average velocity $\langle v \rangle$ *vs.* f_m, at the positions of 2 um and 19 um.

shift within a modulation period or the average velocity profile, we know that the maximum net shift or maximum $\langle v \rangle = s_{total} f_m$ occurs at the position next substrates. At z = 2 um, the net fluid displacement within a period of modulation signal and the shifts following the switching ON (S_{on}) or OFF (S_{off}) are shown in Fig. 10.

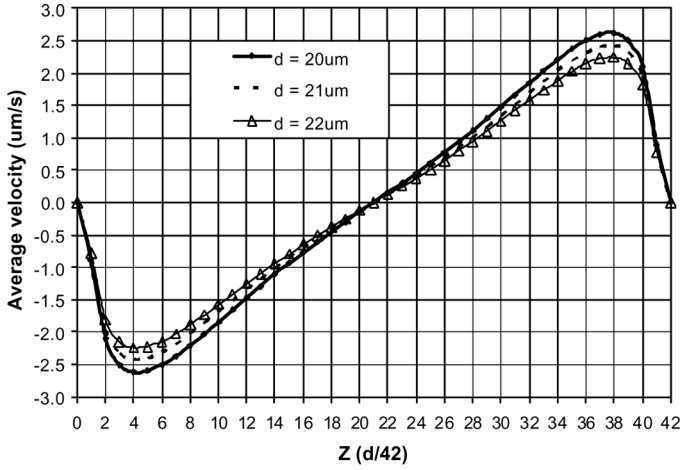

(a)

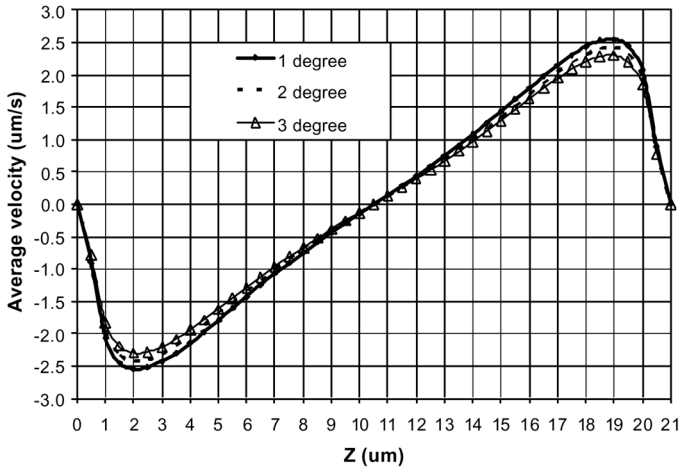

(b)

FIGURE 8 The profiles of average flow velocity $\langle v \rangle$ at $f_m = 10\,\text{HZ}$; (a) for cell thickness 20, 21, and 22 um with a 2° of pretilt angle, (b) for pretilt angle 1°, 2°, and 3° with cell thickness 21 um.

The results show that the flow behavior is different for $f_m << \tau^{-1} = (\tau_{on} + \tau_{off})^{-1} \approx \tau_{off}^{-1} \approx 1\,\text{Hz}$, when $\hat{\mathbf{n}}$ has time to equilibrate, and for $f_m \geq \tau^{-1}$, when $\hat{\mathbf{n}}$ does not equilibrate. In the regime $f_m << \tau^{-1}$, when the field is switched ON, a counterclockwise rotation of $\hat{\mathbf{n}}$ causes a flow with $v_{on}(0 < z < h/2) > 0$ and $v_{on}(h/2 < z < h) < 0$

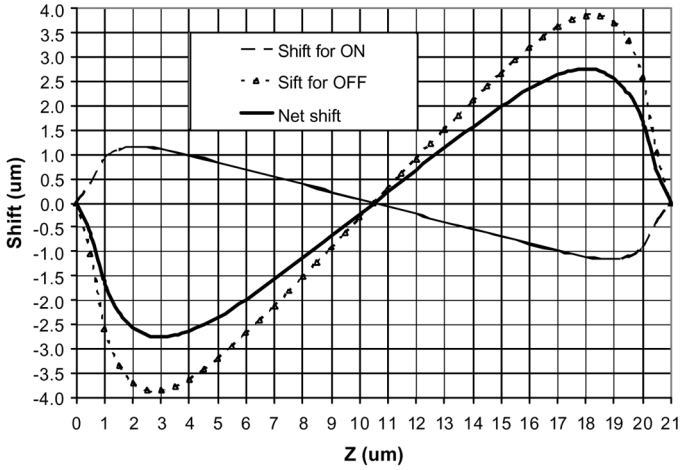

(a)

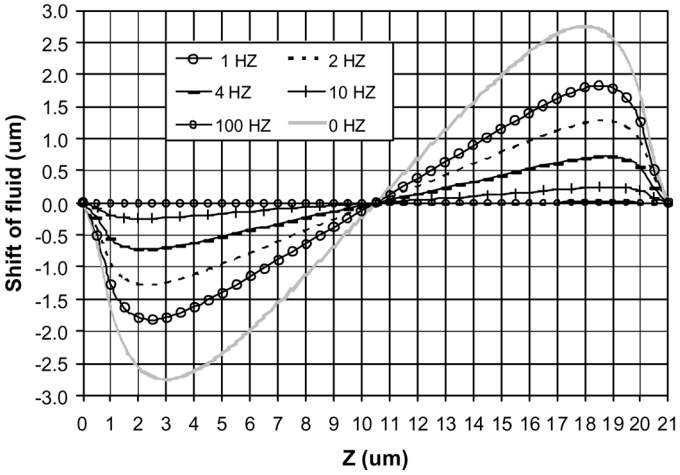

(b)

FIGURE 9 Shift of liquid crystal fluid; (a) shifts in the process of switching ON or OFF, (b) the net shift within a modulation period.

(see Fig. 3a). With time, this flow gradually vanishes. The symmetry $v(z) = -v(h-z)$ allows us to discuss the bottom half only. From Fig. 9a and Fig. 10 we know that the flow-produced displacement $s_{on}(0 < z < h/2) > 0$ is maximum, $s_{on} \approx 1.2\,\mu\text{m}$, at $z \approx 2\,\mu\text{m}$. When the field is switched OFF, the displacement is larger and of opposite sign,

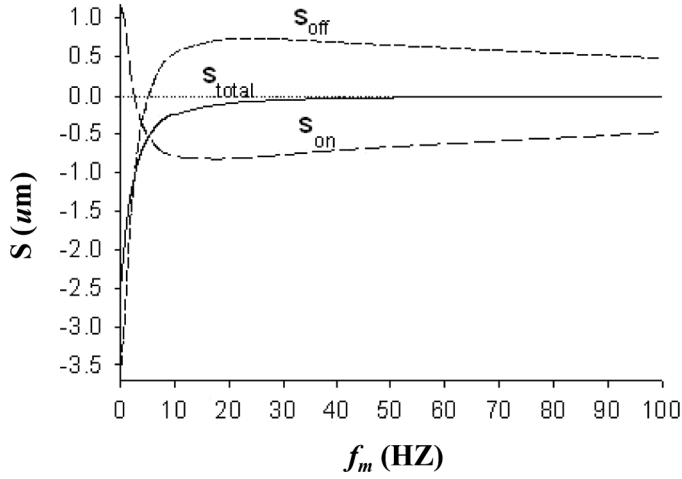

FIGURE 10 Displacement following the switch ON (s_{on}), switch OFF (s_{off}), and during an entire cycle, ON+OFF (s_{total}), at $z = 2\,\mu m$.

$s_{off} \approx -3.7\,\mu m$ for $z \approx 2\,\mu m$. The total displacement per one cycle is negative, $s_{total} = s_{on} + s_{off} \approx -2.5\,\mu m$. For a low f_m, the average velocity of the fluid $\langle v \rangle = s_{total} f_m$ increases linearly with f_m (Fig. 7b). When $f_m \geq \tau^{-1}$, equilibration after each ON and OFF switch is not complete, and the picture is very different. Both s_{on} and s_{off} initially become shorter and then switch signs, but their sum $s_{total} = s_{on} + s_{off}$ remains negative (Fig. 10). In the limit $f_m \to \infty$, small back and forth reorientations cancel each other so that $\langle v \rangle \to 0$ (see Fig. 7b). The dependence $\langle v \rangle (f_m)$ is non-monotonous, with $\langle v \rangle \to 0$ for low and high f_m's and a maximum for an intermediate f_m.

5. CONCLUSIONS

We have shown the whole dynamic process of director and flow for a nematic liquid crystal in the modulated electric field. We quantitatively describe flow velocity, fluid shift, and the dynamic behavior of the director. We also give the net flow velocity and the fluid displacement in a modulated period. Especially, we show an important phenomenon, reverse switch, for nematic liquid crystals in the modulated electric field, which is never mentioned before. The reverse switch and the corresponding reverse flow may be very crucial for understanding dynamics of nematic liquid crystals with complicated switching schemes.

In the calculation of liquid crystal flow and dynamic behavior of director, the used parameters of materials are dependent on the temperature. From [18] we know that elastic constants, dielectric anisotropy, and Leise coefficients have considerable variations with the change of temperature. This may significantly affect switching dynamics of liquid crystals and lead to obvious variation in backflow profile.

REFERENCES

[1] van Doorn, C. Z. (1975). *J. Appl. Phys.*, *46*, 3738.
[2] Berreman, D. W. (1975). *J. Appl. Phys.*, *46*, 3746.
[3] van Doorn, C. Z. (1975). *J. Phys. (Paris)*, *36*, C1-261.
[4] Gerritsma, C. J., van Doorn, C. Z., & van Zanten, P. (1974). *Phys. Lett.*, *A48*, 263.
[5] Van Sprang, H. A. & Koopman, H. G. (1988). *J. Appl. Phys.*, *64*, 4873.
[6] Wohler, H. & Becker, M. E. (1993). *SID 93 Digest*, 650.
[7] Qian, Tie-Zheng, Xie, Zhi-Liang, Kwok, Hoi-Sing, & Sheng, Ping (1997). *Appl. Phys. Lett.*, *71*, 596.
[8] Kelly, J., Jamal, S., & Cui, M. (1999). *J. Appl. Phys.*, *86*, 4091.
[9] Ruan, L. Z. & Sambles, J. R. (2002). *J. Appl. Phys.*, *92*, 4857.
[10] Ruan, L. Z. & Sambles, J. R. (2003). *Phys. Rev. Lett.*, *90*, 168701.
[11] Jewell, S. A. & Sambles, J. R. (2003). *Appl. Phys. Lett.*, *82*, 3156.
[12] Jewell, S. A. & Sambles, J. R. (2004). *Appl. Phys. Lett.*, *84*, 46.
[13] Bos, P. J. & Beran, K. R. (1984). *Mol. Cryst. Liq. Cryst.*, *113*, 329.
[14] Walton, H. G. & Towler, M. J. (2000). *Liq. Cryst.*, *27*, 1329.
[15] Cheng, Hongfei & Gao, Hongjin (2001). *Liq. Cryst.*, *28*, 1337.
[16] Chen, Shu-Hsia & Yang, Chiu-Lien (2002). *Appl. Phys. Lett.*, *80*, 3721.
[17] Brimicombe, P. D. & Raynes, E. P. (2005). *Liq. Cryst.*, *32*, 1273.
[18] Wang, Haiying etc., (2006). *Liquid Crystals*, *V33*(1), 91–98.
[19] Ericksen, J. L. (1960). *Arch. Ration. Mech. Analysis*, *4*, 231.
[20] Ericksen, J. L. (1966). *Phys. Fluids*, *9*, 1205.
[21] Leslie, F. M. (1966). *Quart. J. Mech. Appl. Mah.*, *19*, 357.
[22] Leslie, F. M. (1968). *Arch. Ration. Mech. Analysis*, *28*, 265.
[23] Parodi, O. (1970). *J. Phys. (Paris)*, *31*, 581.
[24] De Jeu, W. H. (1980). *Physical Properties of Liquid Crystalline Materials*, Gordon and Breach Science Publishers: New York.